BNL-103695-2014-TECH
AGS/RHIC/SN 070;BNL-103695-2014-IR

# The simulation of Siberian Snakes based on calculated three dimensional magnet field

X. Meiqin

December 1997

Collider Accelerator Department
**Brookhaven National Laboratory**

**U.S. Department of Energy**
USDOE Office of Science (SC)

## DISCLAIMER

Alternating Gradient Synchrotron Department
Relativistic Heavy Ion Collider Project
BROOKHAVEN NATIONAL LABORATORY
Upton, New York 11973

*Spin Note*

**AGS/RHIC/SN No. 070**

# The simulation of Siberian Snakes based on calculated three dimensional magnet field

X. Meiqin, T. Katayama
(Center for Nuclear Study, The University of Tokyo/RIKEN)

December 3, 1997

# The simulation of Siberian Snakes based on calculated three dimensional magnetic field

Xiao Meiqin T. Katayama

( Center for Nuclear Study, The University of Tokyo/RIKEN)

## 1. Introduction

As a special kind of transport elements in storage ring, Siberian Snakes in RHIC, which consist of four right-handed helical dipole magnets, are expected to rotate spin direction of polarized proton to 180°, and should not affect the beam orbit at the same time, the axis of spin precession should make an angle $\phi = \pm 45°$ too[1][2]. However, the problem is that actually they can not make the spin direction rotate 180° perfectly, also the fringing magnetic field will affect the beam trajectories.

The simulation in Siberian Snakes based on analytical formulation (such as Blewett-Chasman formula) of magnetic field had been well done[3]. For better representation of the real Snakes in RHIC, which are still under the construction, the simulation based on three dimensional magnetic field map is needed. The work had been started by A.U.Luccio[4], but two main problems still remain on the optimization of the spin matrices and of the orbit matrices for the Snakes, they are:

(1) Numerical spin matrices should be unitary,

(2) Orbit matrices should be symplectic, essentially to preserve beam emittance, among other motion integration.

On the other hand, the results of magnetic field measurement for the prototype of a helical magnet was well agreed with those of three dimensional numerical calculation by TOSCA[5]. It was encouraged to work further based on calculated magnetic field map, and to look for different methods to solve the problems mentioned above.

## 2. The methods for simulation

### 2.1 The equations of orbit motion and spin rotation

In Coordinate system of Fig.1, the Lorentz orbit motion equations are

$$\frac{ds}{ds} = 1 \tag{1}$$

$$\frac{dx}{ds} = x' = u \tag{2}$$

$$\frac{dy}{ds} = y' = v \tag{3}$$

$$\frac{du}{ds} = w \cdot [uvB_x - (1+u^2)B_y + vB_s] \tag{4}$$

$$\frac{dv}{ds} = w \cdot [(1+v^2)B_x - uvB_y - vB_s] \tag{5}$$

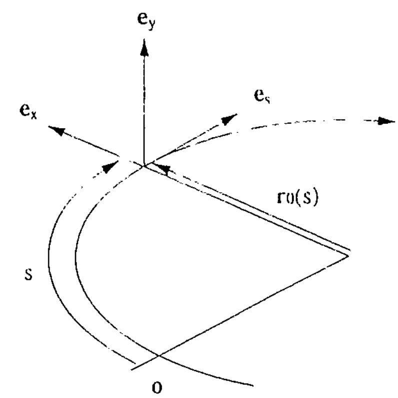


Fig. 1 Coordinate system

where $w = \dfrac{e \cdot (u^2 + v^2 + 1)^{\frac{1}{2}}}{m_0 \gamma V}$, $V$ is the velocity of charged particle. $B_x$, $B_y$, and $B_s$ are the components of magnetic field in x, y and s direction respectively.

The equations of spin precession[6] are

$$\frac{dS_x}{ds} = S_s P_y - S_y P_s \tag{6}$$

$$\frac{dS_y}{ds} = S_x P_s - S_s P_x \tag{7}$$

$$\frac{dS_s}{ds} = S_y P_x - S_x P_y \tag{8}$$

where

$$P_x = \frac{h}{B\rho} \cdot [(1+G\gamma)(-uB_s + (1+v^2)B_x - uvB_y) + (1+G)u(uB_x + B_s + vB_y)]$$

$$P_y = \frac{h}{B\rho} \cdot [(1+G\gamma)(-vB_s + (1+u^2)B_x - uvB_y) + (1+G)v(uB_x + B_s + vB_y)]$$

$$P_s = \frac{h}{B\rho} \cdot [(1+G\gamma)(-uB_x - vB_y + (u^2 + v^2)B_y) + (1+G)(uB_x + B_s + vB_y)]$$

$$h = \frac{1}{\sqrt{x'^2 + y'^2 + 1}} = \frac{1}{\sqrt{u^2 + v^2 + 1}}, \quad B\rho = \frac{m_o \gamma V}{e}.$$

Four-order Runge-Kutta method in Cartesian Coordinates was used to integrate the equations (1) - (8) in this simulation. In order to calculate the axis of spin precession, another three equations with the same form of (6)-(8) were used[7]

$$\frac{dS_x^A}{ds} = S_s^A P_y - S_y^A P_s \tag{9}$$

$$\frac{dS_y^A}{ds} = S_x^A P_s - S_s^A P_x \tag{10}$$

$$\frac{dS_s^A}{ds} = S_y^A P_x - S_x^A P_y \tag{11}$$

The idea is the following:

If a spin vector $\vec{S}$ precesses from $\vec{S}_o$ to $\vec{S}_f$ (see Fig. 2.1), the axis of precession must belong to the plane π bisecting the ($\vec{S}_o$ , $\vec{S}_f$ ) angle. The axis is then perpendicular to the vector $\delta\vec{S} = \vec{S}_f$ - $\vec{S}_o$. If we repeat the same argument for a second spin orientation $\vec{S}^A$, the axis must be also perpendicular to $\delta\vec{S}^A = \vec{S}_f^A - \vec{S}_o^A$. The axis of procession $\vec{S}$ is therefore perpendicular both to $\delta\vec{S}$ and to $\delta\vec{S}^A$. Then

$$\vec{\sigma} = \delta\vec{S} \times \delta\vec{S}^A$$

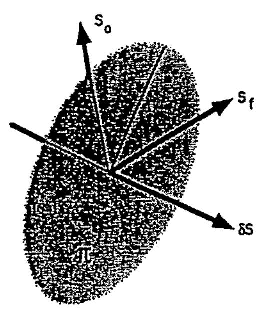


Fig. 2.1 To find the axis of precession

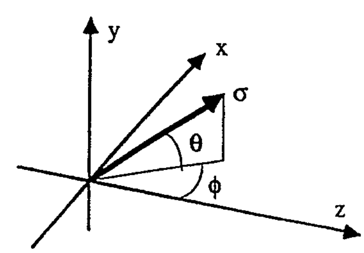


Fig. 2.2 Angles of the axis of precession
φ, horizontal, θ, vertical

The angle are defined as (see Fig. 2.2)

$$tag\phi = \frac{\sigma_x}{\sigma_z}, \qquad tag\theta = \frac{\sigma_y}{\sqrt{\sigma_x^2 + \sigma_z^2}}$$

### 2.2 The interpolation of magnetic field

The magnetic field distribution in three components $B_x$, $B_y$ and $B_s$ of a helical magnet at Cartesian grid $x = x_i$, $y = y_j$ and $s = s_k$ was given. The interpolation for this map was divided into two steps:

(1) Fitting on the (x, y) plane ( $s = s_k$ )

Bicubic spline function method was used to fit $B_x(x,y,s_k)$, $B_y(x,y,s_k)$, $Bs(x,y,s_k)$ (k=1,2,... L) and their derivatives in Cartesian Coordinates ,

$$B_x(x,y,s_k) = \sum_{k,l=1}^{4} A_{x\,ijkl}(x,y)(x-x_i)^{k-1}(y-y_j)^{l-1}$$

$$B_y(x,y,s_k) = \sum_{k,l=1}^{4} A_{y\,ijkl}(x,y)(x-x_i)^{k-1}(y-y_j)^{l-1}$$

$$B_s(x,y,s_k) = \sum_{k,l=1}^{4} A_{s\,ijkl}(x,y)(x-x_i)^{k-1}(y-y_j)^{l-1}$$

$$x_i \le x \le x_{i+1}\,, \quad y_j \le y \le y_{j+1}$$

$$(\,i=1, 2,...m-1, j=1,2,...n-1)$$

Where the coefficients $A_{ijkl}$ can be determined by one-dimensional cubic spline function, and the corresponding boundary conditions

$$\frac{\partial B_x(x,y_j,s_k)}{\partial x}(x = x_1, x_m; j = 1,2,...n)$$

$$\frac{\partial B_x(x_i,y,s_k)}{\partial y}(y = y_1, y_n; i = 1,2,...m)$$

$$\frac{\partial^2 B_x(x,y,s_k)}{\partial x \partial y}(x = x_1, x_m; y = y_1, y_n)$$

could be calculated by two-dimensional 3 - points Lagrangian function

$$B_x(x,y,s_k) = \sum_{i,j=1}^{3}[\prod_{\substack{m,n-1\\ m\neq i\\ n\neq j}}^{3}(\frac{x-x_m}{x_i-x_m})(\frac{y-y_n}{y_j-y_n})] \bullet B_x(x_i,y_j,s_k)$$

(2) fitting in s - the third direction

Spline function method was used again to fit the coefficients on the plane (x, y) $A_{ijkl}(s_1)$, $A_{ijkl}(s_2)$,....$A_{ijkl}(s_l)$ ,

$$SA(s)=K_{0i}+K_{1i}(\Delta s)+K_{2i}(\Delta s)^2+K_{3i}(\Delta s)^3$$

where $\Delta s=s-s_i$

$K_{0i}$, $K_{1i}$, $K_{2i}$, $K_{3i}$ could be calculated by one dimensional spline function fitting.

## 3. The construction of field distribution for full Snakes and Program SSTRAN

Two sets of magnetic field maps on Cartesian grid with 5 mm (named Map827.grid) and with

2.5 mm step (named Map827fine.grid) of half helical magnet length (s=0 ~ L/2) and half space (y≥0,y=0~4 cm) was provided by Dr. M. Okamura. The magnetic field on axis (x=0,y=0) is given in Fig 3 .Then for the region of y< 0, the following symmetrical conditions are used:

$$B_x(x,-y,s)=B_x(x,y,s)$$

$$B_y(x,-y,s) = B_y(-x,y,s)$$

$$B_s(x,-y,s) = -B_s(-x,y,s)$$

For another half length (s=-L/2 ~ 0), the symmetrical conditions are

$$B_x(-x,y,-s) = -B_x(x,y,s)$$

$$B_x(-x,y,-s) = B_y(x,y,s)$$

$$B_s(-x,y,-s) = -B_s(x,y,s).$$

The field distribution of other three helical magnets takes as follows:

$$B2=-BCOEF *B1 \qquad (12)$$

$$B3=-B2$$

$$B4=-B1$$

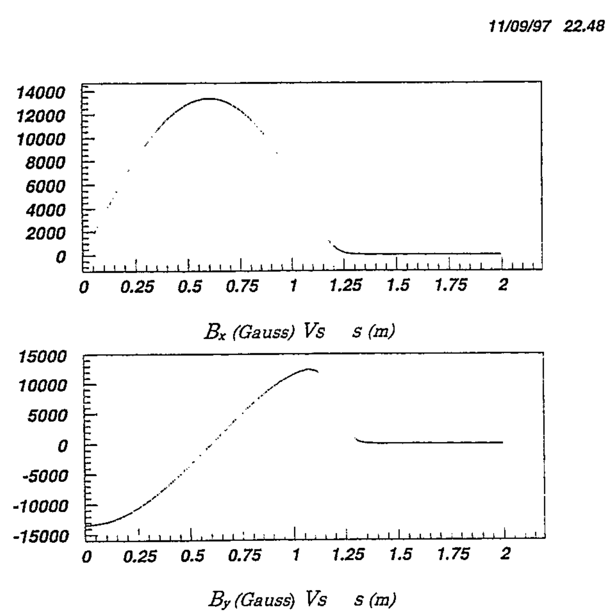


Fig. 3 The magnetic field distribution of Map827.grid on axis (x=0,y=0)

BCOEF in equation (12) is the ratio of the magnetic field strength of the second helical magnet to that of the first one. The constructed field distribution based on Map827.grid on the axis (x=0,y=0) for full Sakes is given in Fig.4.

Program SSTRAN for integrating the equation (1)-(11) based on the calculation methods discussed above was written in FORTRAN .

## 4. Simulation Results

### 4.1 Maxwellian property checking

By using Map827.grid and Map827fine.grid, the interpolated magnetic field from Map827.grid was compared with that directly from Map827fine.grid, the difference between them is within $10^{-5}$. Two magnetic field maps was checked to see how well they satisfy the Maxwell equations

$$\vec{\nabla}\cdot\vec{B} = \frac{\partial B_x}{\partial x} + \frac{\partial B_y}{\partial y} + \frac{\partial B_s}{\partial s} = 0$$

$$\vec{\nabla}\times\vec{B} = \left(\frac{\partial B_s}{\partial y} - \frac{\partial B_y}{\partial s}\right)\vec{i} + \left(\frac{\partial B_x}{\partial s} - \frac{\partial B_s}{\partial x}\right)\vec{j} + \left(\frac{\partial B_y}{\partial x} - \frac{\partial B_x}{\partial y}\right)\vec{k} = 0$$

too. The first derivatives were directly calculated by the coefficients of spline function $A_{ijkl}$ , the results were listed in table 1. It was seen from Table 1 that the scale B is well satisfied ($10^{-6}$) in the region around the axis, the error of curl B mainly comes from $(\vec{\nabla}\times\vec{B})_x$, it may be due to small value of Bs and rapid change with y.

Table 1. The results of Maxwellian property checking on Map827.grid

| Point coordinates (m) | Magnetic field strength (T) | $\vec{\nabla}\cdot\vec{B}$, $\vec{\nabla}\times\vec{B}$ (T/m) |
|---|---|---|
| Fringing point: (0., 0., 0.02) | Bx=0.0698596<br>By=1.33392<br>Bs=0.000000145 | $\vec{\nabla}\cdot\vec{B} = 4.5709596E-6$<br>$(\vec{\nabla}\times\vec{B})_x = -6.304323E-3$<br>$(\vec{\nabla}\times\vec{B})_y = 4.0081994E-3$<br>$(\vec{\nabla}\times\vec{B})_s = -9.4958265E-5$ |
| inside point: (0. 0. 0.15) | Bx=0.511353<br>By=-1.23405<br>Bs=0.000000839 | $\vec{\nabla}\cdot\vec{B} = 4.9906576E-6$<br>$(\vec{\nabla}\times\vec{B})_x = -2.0883111E-2$<br>$(\vec{\nabla}\times\vec{B})_y = -4.0178569E-3$<br>$(\vec{\nabla}\times\vec{B})_s = -2.1633758E-4$ |
| point far from axis (-2.5, 2.5, 0.15) | Bx=0.51472201<br>By=-1.24078<br>Bs=-0.047527853 | $\vec{\nabla}\cdot\vec{B} = 7.366029E-3$<br>$(\vec{\nabla}\times\vec{B})_x = -2.2103902E-2$<br>$(\vec{\nabla}\times\vec{B})_y = 2.6094199E-3$<br>$(\vec{\nabla}\times\vec{B})_s = -4.9999588E-2$ |

### 4.2 Optimized BCOEF

The ray with initial conditions of $(x_o, x_o', y_o, y_o')$ = (0. 0. 0. 0.) and $(S_{ox}, S_{oy}, S_{os})$ = ( 0 1 0 ) was traced through the full Snakes and optimized for BCOEF based on numerical calculated magnetic field of Map827.grid. BCOEF was adjusted automatically so as to get the final orbit angle $x_e'$, $y_e'$ as small as possible and $S_{ey}$ as closed to -1 as possible ( spin direction turn over 180°). Take the fringing magnetic field into account, the magnetic field from 0 ~ 1.312 m ( this is the length of Yoke) was taken from Map827.grid. The optimized BCOEF obtained is 3.09557299 when the amplitude of the field strength of the first magnet is 1.33626 T. The results of the final orbit and spin precess were listed in table 2 together with those based on Blewett-Chasman field formulas[8] for comparison, the trajectory and spin procession in full snake were shown in Fig. 5 and Fig.6 respectively.

Table 2. The results of the trajectory with initial condition of $(x_o, x_o', y_o, y_o')$ = (0. 0. 0. 0.) and $(S_{ox}, S_{oy}, S_{os})$ = ( 0 1 0 ) when the field strength of the second magnet is at optimized value.

| Filed<br>Results | Map827.grid | Blewett-Chasman formula |
|---|---|---|
| $B_{m1}$ (T) | 1.336260 | 1.336260 |
| $B_{m2}$ (T) | 4.136490 | 3.987906 |
| x (mm) | 0.24 | -17.557 |
| x'(mrad.) | 0.01111 | -1.58361 |
| y (mm) | -0.46 | 2.0 |
| y'(mrad.) | -0.08429 | 0.15085 |
| Sx | 0.01553612 | -0.06402582 |
| Sy | -0.99973410 | -0.99512058 |
| Ss | -0.01704195 | 0.07528736 |
| φ(°) | 51.47374108 | 45.98502244 |
| θ(°) | -0.04410307 | 0.99667815 |

### 4.3 spin matrix

With the same initial orbit of $(x_o, x_o', y_o, y_o')$ = (0. 0. 0. 0.) , three representative rays with initial spin $\vec{S}_o$=(1 0 0) , (0 1 0) and (0 0 1) respectively were traced, then spin matrix could be directly got by the final precessed spin. At the optimum value of BCOEF=3.09557299, that is B1=1.33626 T, B2=4.136490 T, the spin matrix

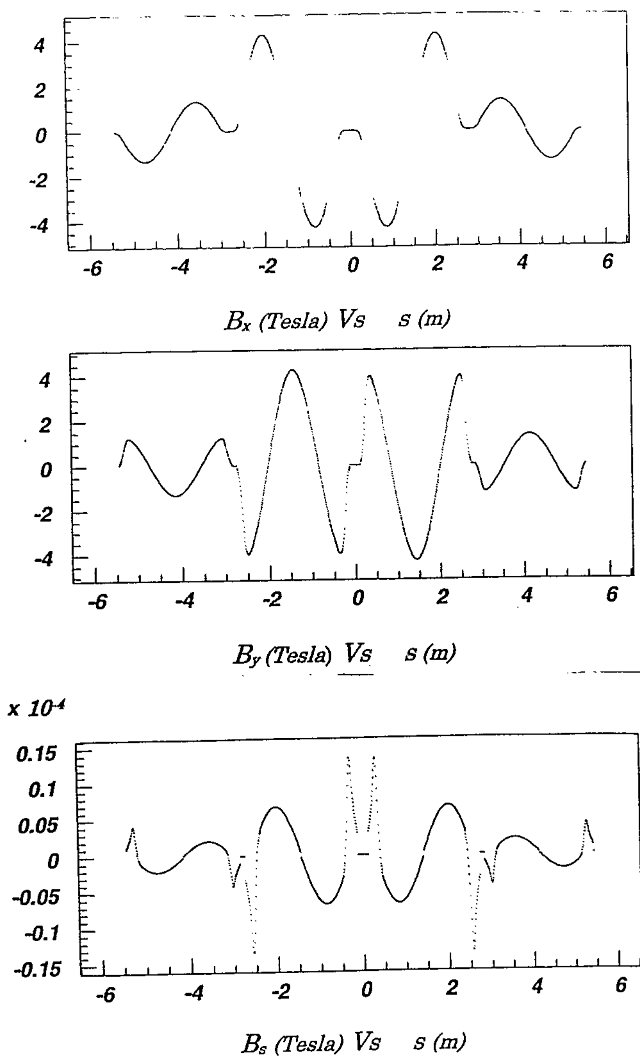


Fig. 4 The constructed field distribution of full Snakes on axis (x=0, y=0)

$$M_S = \begin{bmatrix} 0.22415978 & -0.01312770 & 0.97446405 \\ 0.01553612 & -0.99973410 & -0.01704195 \\ 0.97442862 & 0.01895950 & -0.22389618 \end{bmatrix}$$

The determinant of $Ms$: $\det[Ms] = 1.00000014777028$

$|\det[Ms]-1| = 1.4777028E-7$

The dependence of the matrix elements on particle position and angle was investigated too. The calculation was repeated for different values of $(x_o, x_o', y_o, y_o')$. The spin process of some of the rays with large r (r>3.0cm) rotate unregularly, but most of them turn out to be very close to each other, and the determinant of their matrices have the same order (1.E-7).

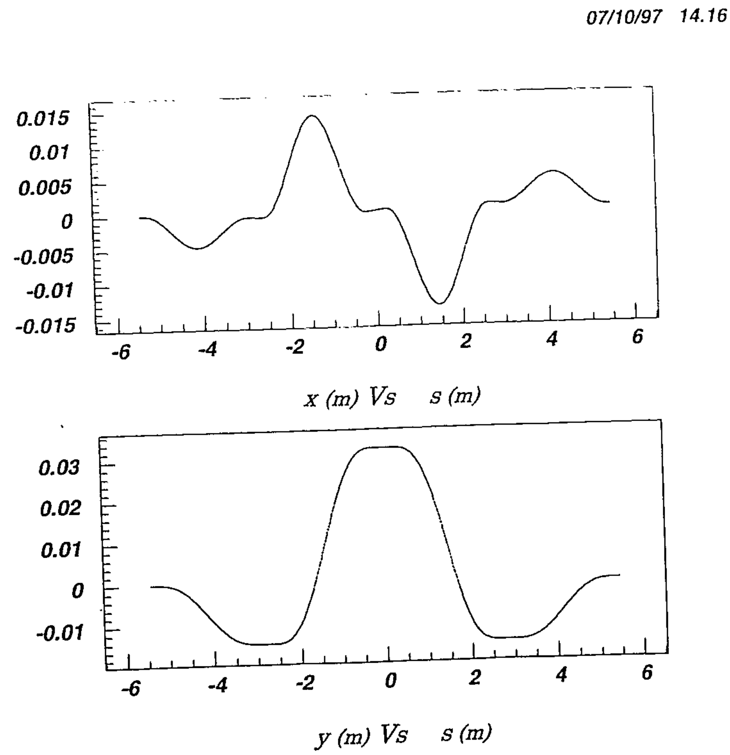


Fig. 5 The trajectory of the ray with $(x_o, x_o', y_o, y_o') = (0.\ 0.\ 0.\ 0.)$

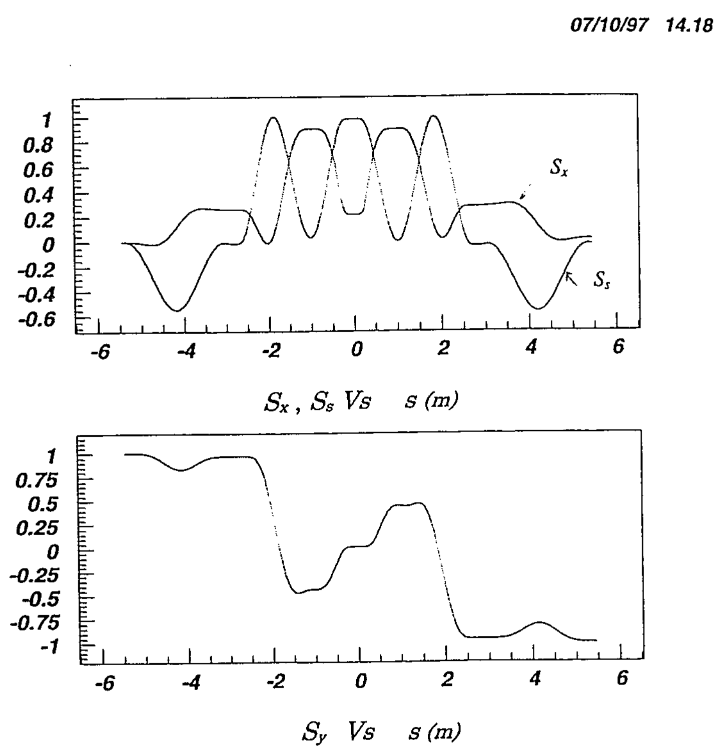


Fig. 6 The spin precession of the ray with $(S_{ox}, S_{oy}, S_{os}) = (0\ 1\ 0)$

### 4.4 orbit matrix

The calculation of orbit matrix $M_T$ is more complicated than that of spin matrix. To calculate $M_T$, a certain number of rays, whose initial conditions were generated by random with Gaussian distribution in the components of $(x_o, x_o', y_o, y_o')$, were tracked. By solving a system of algebraic equations between the final and the initial coordinates of the same ray, a transformation expressed as a power expansion truncated to a pre established degree can be found. In this simulation, we are interested in a 0.th order 4×4 matrix. The problem has the same sense of general linear least squares, the solutions by use of the *normal equations* [9] was taken to get elements of the matrix .

It was found that the results largely depend on the number of the rays traced, The more the rays traced, the better the results.

After the number of the rays over 16, the matrix calculated is getting stable, the following is the result from 16 rays traced,

$$M_{or} = \begin{bmatrix} 0.99391892 & 10.82810815 & -0.01694592 & -0.03364342 \\ -0.00429513 & 0.96566983 & 0.00604201 & -0.00743476 \\ 0.00061034 & 0.16304712 & 0.98440460 & 10.67164840 \\ 0.00060338 & 0.06262435 & -0.00489109 & 0.94845089 \end{bmatrix}$$

The determinant of $M_{or}$: $\det[M_{or}] = 0.99508166\text{E}+00$

$|\det[M_{or}]-1| = 4.91834490\text{E}-03$

## 5. Conclusion

One set of methods have been setup for simulation in Siberian Snakes, and the results for numerical calculated magnetic field of Map827.grid is good, but further work should be done in next step.

## References

[1] K.Brown (BNL),et al. Conceptual Design for the Acceleration of Polarized Protons in RHIC. Spin Note AGS/RHIC/SN No.001.January 19,1996.

[2] T. Katayama, Spin Dynamics in Synchrotron and Storage Ring, November,1995.

[3] H.Wu, et al. Numerical and Analytic Studies on Siberian Snake. Spin Note AGS/RHIC/SN No. 025. April 29,1996.

[4] A.U.Luccio, Field Map Generated Matrices for Spin Tracking. Spin Note AGS/RHIC/SN No.

041. November 5,1996.

[5] M .Okamura, The Hall Probe Measurement and Calculation of the Half Length Helical Dipole Magnet. Spin Note AGS/RHIC/SN No. 060, August 20,1997.

[6] V.Bargmann, Louis Michel and V.L.Telegdi, Procession of the Polarization of Particles Moving in a Homogeneous Electromagnetic Field. Physical Review Letters. Vol. 2, No. 10. May 15,1959.

[7] A.U.Luccio, Numerical Studies of Siberian Snakes and Spin Rotators for RHIC. Spin Note AGS/RHIC/SN No. 008. January 19,1996.

[8] J. P. Blewette and R. Chasman, Orbits nd fields in the helical wiggler. Journal of Applied Physics, Vol.48, No. 7,July 1977.

[9] W.H.Press et al. Numerical Recipes in FOTRAN,The Art of Scientific Computing Second Edition. Cambridge University Press, 1992.